Assessment of novel acoustic liners for aero-engine applications with sheared mean flow

Suresh Palani*, Paul Murray† and Alan McAlpine‡
Institute of Sound and Vibration Research, University of Southampton, Southampton, SO17 1BJ, United Kingdom

Kylie Knepper§
The Royal Netherlands Aerospace Centre, Voorsterweg 31, 8316 PR Marknesse, The Netherlands

Christoph Richter¶
Rolls-Royce Deutschland Ltd & Co KG, Dahlewitz, Eschenweg 11, 15827 Blankenfelde-Mahlow, Germany

Abstract

In this paper the performance of two novel broadband liners for aero-engine applications is assessed in the presence of both high sound pressure level and grazing flow. The novel liner configurations include a slanted porous septum concept with varying percentage open areas, and a MultiFOCAL (MULTIple FOlded CAvity Liner) concept. In-duct liner insertion loss predictions and measurements for both downstream and upstream sound propagation are presented, with the results compared to an optimised conventional single-degree-of-freedom perforate liner. Both the novel liners are predicted and measured to provide improved broadband attenuation for downstream propagation, with excellent agreement seen between the measurement and prediction. For downstream sound propagation, a uniform flow model (convected wave equation) with the standard Ingard–Myers boundary condition is shown to predict the liner attenuation accurately, indicating that the boundary effects can be neglected for the downstream case. For upstream sound propagation, the insertion loss predictions and measurements highlight the importance of accounting for boundary-layer refraction in the numerical modelling. Thus, the linearised Euler equations are used to model the effect of the boundary layer on the predicted liner attenuation for upstream propagation.

I. Introduction

Acoustic panels are known to provide a significant contribution to the reduction of fan noise that is radiated from an aircraft nacelle. Acoustic liners are installed typically in the engine inlet, bypass, and core ducts. Their deployment must be balanced by weight and drag concerns, and by the geometric limitations imposed by high-bypass-ratio engines. The spectrum of the noise source from modern fans is more broadband than that of earlier designs. Consequently, more effective designs of acoustic liners are required in order to attain the desired levels of noise reduction, particularly as future large engines are expected to have lower liner length to diameter aspect ratios.

In recent years much research has been devoted to the design of complex cavities to realise a better match to the optimum acoustic impedance for aero-engine noise reduction at lower frequencies. Unconventional liner concepts with novel sound absorbing mechanisms have been studied to achieve close to perfect sound absorption at sub-wavelength frequencies, while maintaining the structural dimensions much smaller than the wavelength of the incident waves. For example, Sugimoto et al. [1] investigated the design and performance of folded cavity liners for turbofan engine inlets. Schiller and Jones [2] developed a broadband liner design concept called a variable depth liner, composed of groups of resonators tuned for different frequencies. When developing such highly effective novel liners, one has to consider not only the effect of liner parameters such as the resistive sheets, cavity geometry, cell depths, and incident sound pressure level, but also the mean flow and boundary-layer effects.

*PhD Candidate, Institute of Sound and Vibration Research (ISVR), S.Palani@soton.ac.uk.
†Principal Research Fellow, Institute of Sound and Vibration Research (ISVR), pm2@isvr.soton.ac.uk.
‡Associate Professor, Institute of Sound and Vibration Research (ISVR), A.McAlpine@soton.ac.uk.
§R&D Engineer Aeroacoustics, The Royal Netherlands Aerospace Centre (NLR).
¶Specialist Acoustics, RRD System Design-Noise, Rolls-Royce Deutschland Ltd & Co KG.

This is the author's version (post-print) of the work that was accepted for publication in the proceedings of the 28th AIAA/CEAS Aeroacoustics Conference held at Southampton, June 2022.
The final version was published in the proceedings of the conference as paper No. 2022-2900. https://doi.org/10.2514/6.2022-2900

The mean-flow boundary layer over the facing sheet of liners has been shown to have a substantial effect on upstream propagation and absorption of sound in ducts [3, 4]. The velocity gradient in the boundary-layer region can be expected to refract the sound field either towards or away from the liner surface depending on its propagation direction with respect to the mean flow. In order to model the sound propagation above the liner in the presence of mean flow, Myers [5] extended the work of Ingard [6] and proposed a boundary condition with the assumption of an infinitely thin boundary layer, known as a vortex sheet. Gabard [7] assessed the influence of boundary-layer refraction on the liner attenuation rate by solving eigenvalue problems for uniform flow with both the Myers [5] and a modified Myers condition [8], with a fixed boundary-layer thickness representative of nacelle conditions. Gabard [7] concluded that the boundary-layer refraction effects cannot be ignored for upstream sound propagation. Furthermore, the accuracy of the liner attenuation rate improved when using the modified Myers condition, with Gabard recommending the use of displacement thickness to characterise the boundary-layer effects.

This paper extends earlier work presented in Ref. [9], which considered liner insertion loss prediction in the presence of uniform flow. The primary aim of this paper is to present the results of a detailed evaluation of two novel liner concepts, named Slanted Septum Core (SSC) and a MULTIple FOlded CAvity Liner (MultiFOCAL), while accounting for the influence of boundary-layer refraction, and the impact of the boundary layer profile. This is achieved by using numerical modeling to predict the liner insertion loss in a flow duct test facility in the presence of a shear flow. The prediction results show that the boundary layer significantly changes the peak insertion loss for the upstream propagation condition, further causing a frequency shift of this peak. Furthermore, the prediction results of both liners indicate a strong function of boundary layer profile and thickness on the attenuation spectra. Particular interest is also put into the design of the liner cavity with complex internal structures, emphasising the optimum liner parameters for achieving maximum insertion loss at moderate sound pressure levels for grazing incidence of multi-modal sound in the presence of flow.

II. Computational model

The computational model is based on the geometry of the Royal Netherlands Aerospace Centre (NLR) flow duct facility. As shown in **Fig. 1a**, the NLR flow duct test section is rectangular with length 1.05 m and cross-sectional area 0.3×0.15 m^2. The test section is flush-mounted into the wind tunnel that connects two reverberation chambers in which the sound power level is measured using a microphone array to determine the insertion loss provided by a lined test section under grazing flow conditions in the presence of high intensity sound waves. The attenuation spectra of candidate liner geometries were determined at the various flow conditions by testing with and without lining material. In addition, experiments were performed with an SDOF perforate liner (NLR reference panel) for reference cases to compare with the novel liner attenuation levels. For the numerical study, a two-dimensional axisymmetric annular duct model, with a 2 m inner radius (R_i) and a 2.3 m outer radius (R_o), is used to represent the longitudinal cross-section of the NLR flow duct test facility. An annular duct model is adopted in order to facilitate the efficient insertion of acoustic modes within the COMSOL[10] finite element (FE) code. It is well known that, in the limit of large hub-to-tip ratio, axisymmetric modes in an annular duct closely approximate the modes in a two-dimensional rectangular duct. A schematic of the annular duct model used in this study is shown in **Fig. 1b**. The duct axis is x and the radial coordinate is r. The model includes unlined (hard-wall) sections of length 1 m either side of a lined section of length L_{lined}. Additionally, the ratio of the length of the lined section to the duct height is approximately 2.8 which is a good representation of a nacelle bypass duct with positive flow Mach numbers [11].

The Linearised Euler Equations (LEE) frequency domain model in COMSOL is used to describe the propagation of the sound field within the duct. The linearised potential flow equation is solved on the boundary, at $x = 0$, on which the broadband noise source is defined. The broadband noise source is modelled by assuming excitation of all cut-on, hard-wall, radial duct modes for the m=0 azimuthal mode at a prescribed frequency[12, 13]. The propagating radial modes are assumed to be uncorrelated, such that the in-duct sound power transmission loss of each mode can be calculated separately, with the assumption of equal energy per mode at the source plane. The sound power loss for different propagating modes at the same excitation frequency can be summed, because of the orthogonality of the mode shape functions, to estimate the total power loss [14]. The sound power of the incident radial modes is set to unity using the intensity formulations of Morfey [15]. A reflection-free condition is defined at the exit plane of the unlined termination section by using a perfectly matched layer (PML) [10].

In the lined section, the wall impedance is modelled using the Ingard–Myers boundary condition [5]. To simulate the NLR's test condition, only the outer wall is lined.

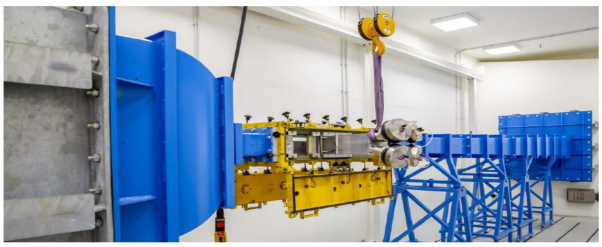

(a) Picture of NLR flow duct facility

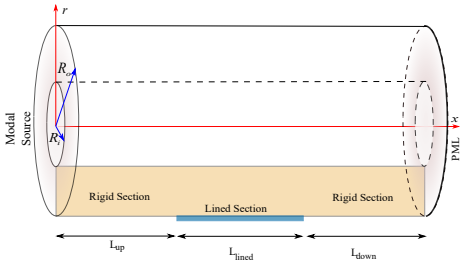

(b) Schematic of the annular duct model

Fig. 1 Experimental and numerical set-up for liner aeroacoustic performance assessment.

III. Broadband novel liners

The two novel liner configurations designed and manufactured for broadband sound attenuation are illustrated in **Fig. 2**. Configuration 1 is a cavity liner with a slanted septum having two different percentage open areas 2a. Configuration 2 is referred to as a Multiple FOlded CAvity Liner (MultiFOCAL) 4, and consists of a set of folded cavities tuned to different acoustic wavelengths. The novel liner concepts are optimised to provide broadband insertion loss in the frequency range of 0.5 to 6 kHz. The cavity depth (Hc) of the novel liners is set nominally to 60 mm to limit the space requirement of the acoustic liners installed inside a turbofan nacelle. Further details of the optimization methodology are provided in Ref. [9, 16].

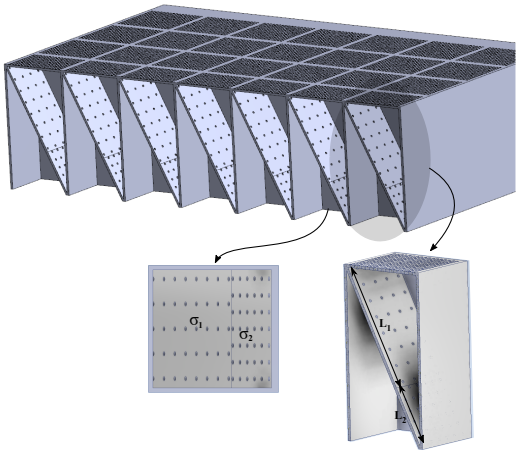

(a) Slanted Septum Core with variable open area

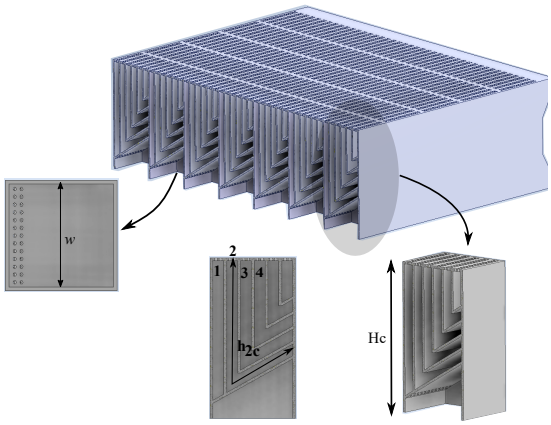

(b) MultiFOCAL Panel

Fig. 2 Schematics of the Slanted Septum Core (SSC) and the MultiFOCAL liner concepts

A laser sintering additive manufacturing method has been used to fabricate the liner panels. The panels were manufactured by the NLR, who also performed insertion loss measurement in the presence of grazing flow. The nominal thickness of the resistive sheets of the liner samples is maintained as 1 mm. Also, the hole diameter of the perforated facing sheet and the core septum is set to 1 mm in order to maximise hole quality. The bottom portion of the liner panels is left open to remove the metal powder trapped inside the liner complex cavities during 3-D printing. Additional novel liner samples were also manufactured by using the Stereolithography (SLA) 3D printing method.

IV. Impedance modelling and measurement

The predicted and measured normal incidence impedance spectra of the slanted septum core and the MultiFOCAL concepts are presented in this section. The impedance predictions were performed using the COMSOL FE model. Pure tone plane waves are normally incident on the liner surface at a targeted sound pressure level ranging from 130 to

150 dB, for frequencies between 100 Hz and 5500 Hz, in steps of 100 Hz. Ref. [16] provides a detailed description of the numerical model used for predicting the liner impedances.

In the finite element model, the interior boundary condition for the perforated layer is given by Equation 1 in Ref.[9] to predict the impedance spectra for each liner configuration. The predicted impedance spectra are compared with those measured using the NLR's high-intensity impedance test set-up. **Fig. 3** shows the NLR normal incidence impedance test set-up.

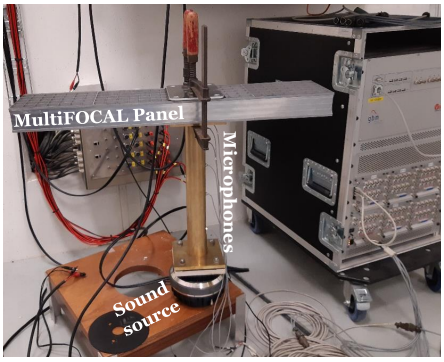

Fig. 3 NLR normal incidence test set-up

The acoustic impedance of the liner panels was measured at eight locations (see Fig. 4), using both tonal and broadband excitations. The overall sound pressure level (OASPL) was increased from 130 to 150 dB, in steps of 5 dB, to evaluate non-linear effects. The tonal measurements were performed for frequencies between 500 and 5000 Hz, in steps of 500 Hz.

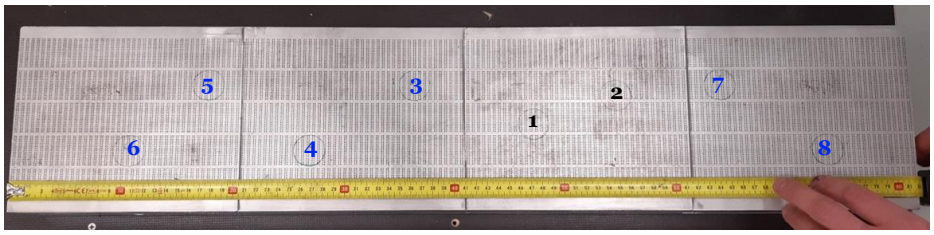

Fig. 4 MultiFOCAL panel marked with the normal incidence impedance test locations

A. Slanted Septum Core

In **Fig. 5**, the impedance prediction model is validated by comparing predicted tonal impedance spectra to the measurements. The percentage open area (POA or σ) of the facing sheet, septum layers 1 and 2 are optimised for maximum insertion loss at Mach = +0.3 and SPL =140 dB (approach type condition). The details of the liner design and optimisation are provided in Refs. [9, 16].

From the pure tone impedance spectra (no grazing flow), it can be seen that the prediction shows good agreement with the measured data. The resistance (red) and reactance (blue) are normalised by the characteristic impedance of air ρc. At 130 dB (see in Fig. 5a), the normalised reactance of this liner configuration crosses zero (towards positive values) at 920 Hz, 2800 Hz, and 5200 Hz. Also, anti-resonances can be seen at 2100 Hz and 4700 Hz. Furthermore, as expected, as the SPL increases, the resistance increases, and the reactance decreases for frequencies away from the anti-resonances (see Fig. 5a & Fig. 5c). The total resistance of the SSC at 150 dB is approximately 0.5 to 1.0 ρc, for frequencies away from the anti-resonances, higher than the corresponding values at 130 and 140 dB. Another important observation is the clear evidence of damping of the anti-resonances at higher SPLs, with the "flattening" of the reactance, leading to improved absorption at higher frequencies. Additionally, it is observed that, for OASPLs of 130 and 140 dB, there are negligible differences between the normal incidence impedance for the tonal and broadband excitation.

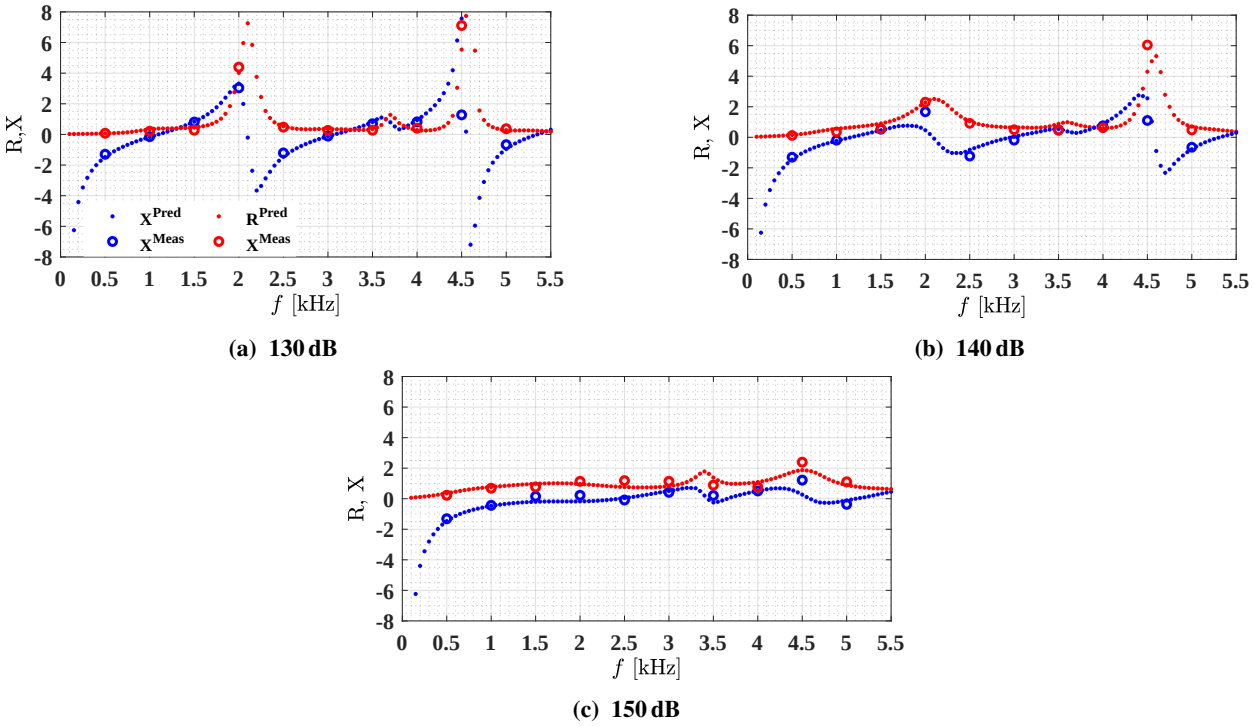

(a) 130 dB **(b) 140 dB**

(c) 150 dB

Fig. 5 Comparison between the predicted (dot) and the measured (hollow circle) tonal response of the SSC liner panel at Mach = 0. Resistance (red color) and Reactance (blue colour).

B. MultiFOCAL

Fig. 6 shows the comparison of the measured and the predicted impedance spectra of the MultiFOCAL liner geometry, using pure tone excitations. As stated earlier, the details of the liner design and optimisation are provided in Refs. [9, 16], and summarised in Table. 1.

In **Fig. 6a**, for pure tone excitation at 130 dB, the normalized reactance is close to zero for most of the frequencies in the range of 0.5 to 5.5 kHz given the combination of six folded cavities with different depths. The resistance of the liner surface is mainly controlled by the septum (septum 1) of segment 1, in addition to the perforated facing sheet. This is because the optimum percentage open area of septum 1 is low compared to the facing sheet of segments 1–6. Hence, the septum has a greater non-linear resistance component at high SPLs.

As in the case for the SSC, comparing the normal incidence impedance spectra using tonal excitation at 130, 140, and 150 dB highlights the influence of sound pressure level on the acoustic properties of the MultiFOCAL configuration. The total resistance of the MultiFOCAL at 150 dB is close to 1.0 ρc, for frequencies away from anti-resonances, higher than the corresponding values at 130 dB. Also, there is again clear damping of anti-resonances with increasing sound pressure level for tonal excitations. Therefore, at 150 dB (Fig. 6c), the six closely packed peaks at lower SPLs are broadened due to damping of the anti-resonances, and flattening the normalised reactance curve towards zero.

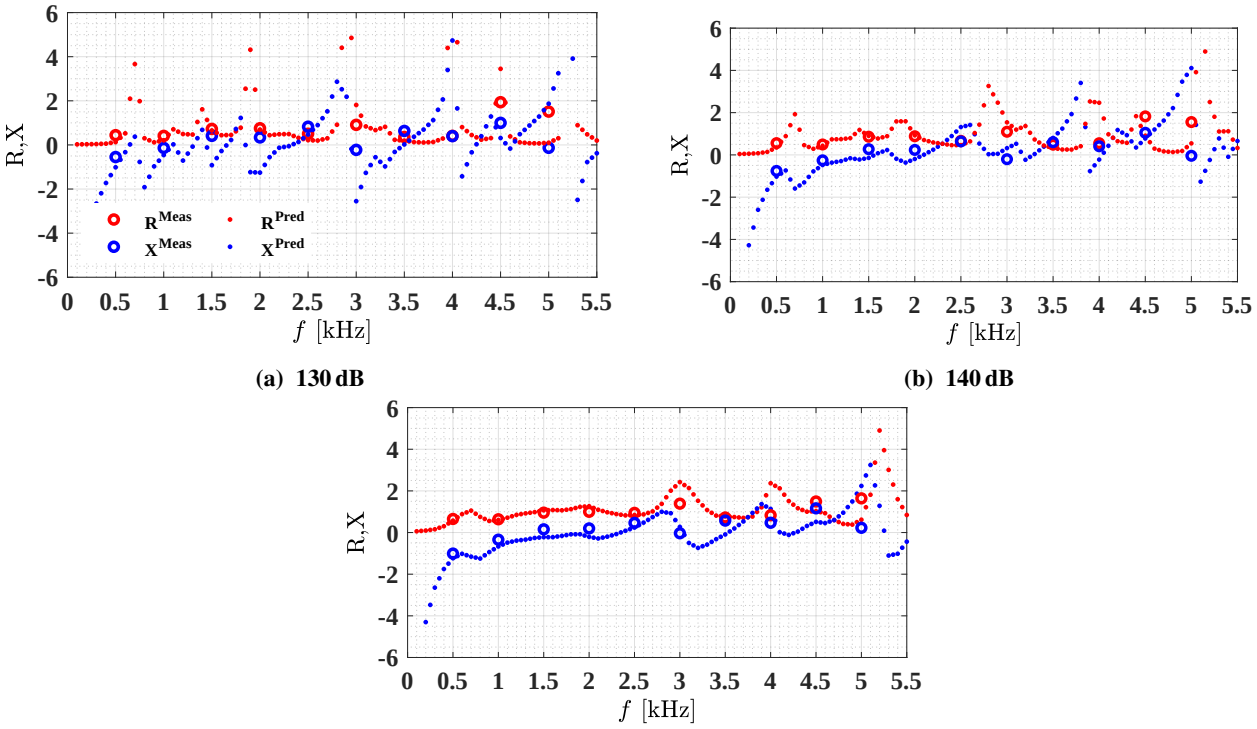

(a) 130 dB

(b) 140 dB

(c) 150 dB

Fig. 6 Comparison between the predicted (dot) and the measured (hollow circle) tonal response of the Multi-FOCAL liner panel at Mach = 0. Resistance (red color) and Reactance (blue colour).

V. Measured insertion loss of SSC and MultiFOCAL liner concepts

In the flow duct facility at the NLR, experiments have been conducted to assess the performance of the new liner concepts (SSC and MultiFOCAL) presented in Section III, with mean flow grazing over the liners at Mach numbers representative of aero-engine operating conditions. For comparison an optimised single-degree-of-freedom (SDOF) perforate liner was also tested as a reference configuration. The geometrical parameters of the liner panels tested at the NLR flow duct facility are summarised in **Table. 1**. The facing sheet POAs are a little higher than optimum as the hole diameter realised from 3D printing is higher than specified. It is noted that one duct wall was lined in all cases.

Table 1 Geometrical parameters of the liners tested at the NLR flow duct facility

Liner Type	Panel Dimension	Facing Sheet POA (%)	Septum 1 POA (%)	Septum 2 POA (%)	Cavity Depth (mm)
SDOF(Perforate)	850 mm × 170 mm	5	-	-	20
SSC	818 mm × 170 mm	27.5	4.7	2	60
MultiFOCAL	818 mm × 170 mm	25.7	2.4	2.9	60

The measured insertion loss is calculated from the difference between the sound power transmission loss with and without the liner, and is given by

$$\mathrm{IL} = \Delta_{\mathrm{PWL}}^{\text{With liner}} - \Delta_{\mathrm{PWL}}^{\text{Without liner}}. \tag{1}$$

Fig. 7 compares the insertion loss at M = 0 for the SSC, MultiFOCAL, and reference SDOF perforate liner configurations. As expected, for frequencies below 1 kHz (see Fig. 7a), both of the novel liner panels show a significant improvement in noise reduction. For frequencies between 0.5 and 0.95 kHz, the slanted septum core provides an insertion loss of at least 4 dB. On the other hand, the MultiFOCAL panel has two peaks in the spectrum between 0.4 and 1 kHz. The first peak occurs at 0.5 kHz, and the second peak at 0.92 kHz, with an insertion loss of 12 dB and 7 dB, respectively. The MultiFOCAL's insertion loss drops a little around 0.7 kHz. This is because the optimum impedance and the maximum

possible insertion loss are very sensitive to small changes in impedance at low frequencies [9]. Additionally, it has been shown in Refs. [9, 11] that the maximum possible insertion loss is more sensitive to changes in impedance at lower frequencies than at higher frequencies.

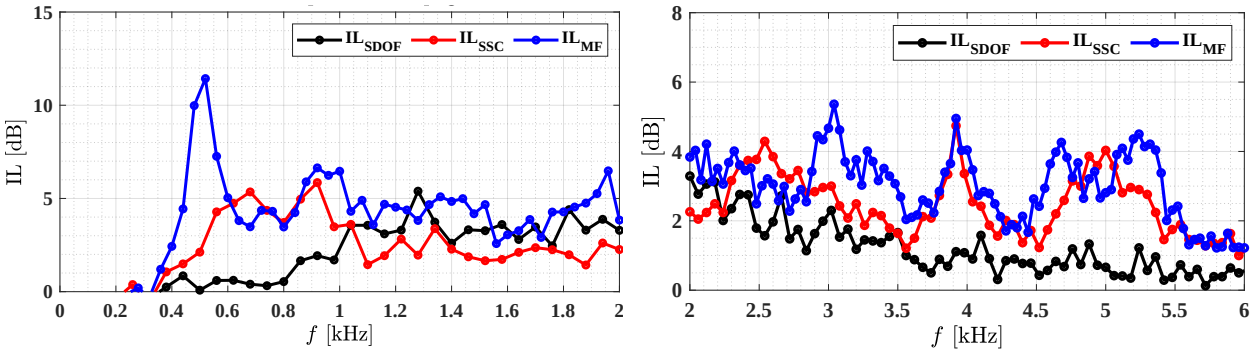

(a) 0.2 to 2 kHz **(b) 2 to 6 kHz**

Fig. 7 Comparison of measured insertion loss at Mach = 0

For frequencies between 1 kHz and 2 kHz, the SSC's insertion loss drops below the SDOF perforate. However, for frequencies above 2 kHz (see Fig. 7b), the insertion loss of the SSC and the MultiFOCAL is at least 2 dB more than the SDOF perforated liner. The insertion loss achieved by the SDOF perforate type liner then decreases gradually with increasing frequency (see Fig. 7b). As the anti-resonance of the SDOF perforate liner is out of the targeted frequency range, there are no dips in the insertion loss below 6 kHz. In general, the acoustic performance of the novel liners at the no flow condition is a net attenuation gain compared to the SDOF perforate type liner. This is not surprising given the relatively low resistance of the perforate liner without flow.

A. Downstream propagation

In this section, the mean flow Mach number is varied from M = 0.3 to 0.7 to determine its impact on liner performance. The acoustic source is broadband, with OASPL = 130 dB. The measured insertion loss for each liner configuration for the downstream sound propagation condition are compared and presented in **Fig. 8**. The liner configurations investigated in this work all have a perforated facing sheet. As a result, these liners have a relatively higher resistance with the mean flow than for cases without flow. Again, for comparison, an SDOF perforate reference liner panel is tested, and the results are presented in Fig. 8 marked by the solid black line.

Ref. [9] provides a detailed description of the optimisation of the liner's design parameter (percentage open area) for maximum sound attenuation at Mach = +0.3 and SPL = 140 dB. The optimisation results, presented in Ref. [9], are based on the installation of the liners on both the top and bottom walls of the NLR flow duct test section. It is noted again that the results presented here are for one side lined.

At Mach = +0.3, and for frequencies between 0.3 and 1.2 kHz, the novel broadband liners with complex cavities demonstrate generally improved attenuation when compared with the conventional SDOF perforate (see **Fig. 8a**). As can be seen from the insertion loss plot in **Fig. 8b**, for frequencies between 1.2 and 6 kHz, the MultiFOCAL performance is comparable or slightly better than the SDOF perforate at all frequencies except at around 2.5-3 kHz. The reason for this is the anti-resonance in the impedance spectrum (between 2.5 kHz and 3 kHz), where the reactance moves from $+3\rho c$ to $-3\rho c$ (see Fig. 6a). Additionally, comparison of Fig. 7a and Fig. 8 shows that for the MultiFOCAL concept, the peak insertion loss at 0.5 kHz has decreased. The SSC liner concept has two strong anti-resonances at 130 dB (see Fig. 5a); therefore, the corresponding insertion loss of this liner has two dips, at around 2.1 kHz and 4.3 kHz, in the targeted frequency range. Also, it should be mentioned that at Mach = +0.3, the signal-to-noise ratio for all liner configurations is well above the acceptable limit for the entire range of frequencies between 0.2 and 6 kHz. Compared to the no-flow condition, the insertion loss peak shifts towards a higher frequency, and is now more broadband for the novel liner configurations, especially for the MultiFOCAL. This once again illustrates the sensitivity of the insertion loss to small changes in optimum impedance and liner impedance at lower frequencies as compared to higher frequencies [9]. Also, as the manufactured POA of the facing sheet of both liners is higher than the design value, the design value would provide a further increase in performance.

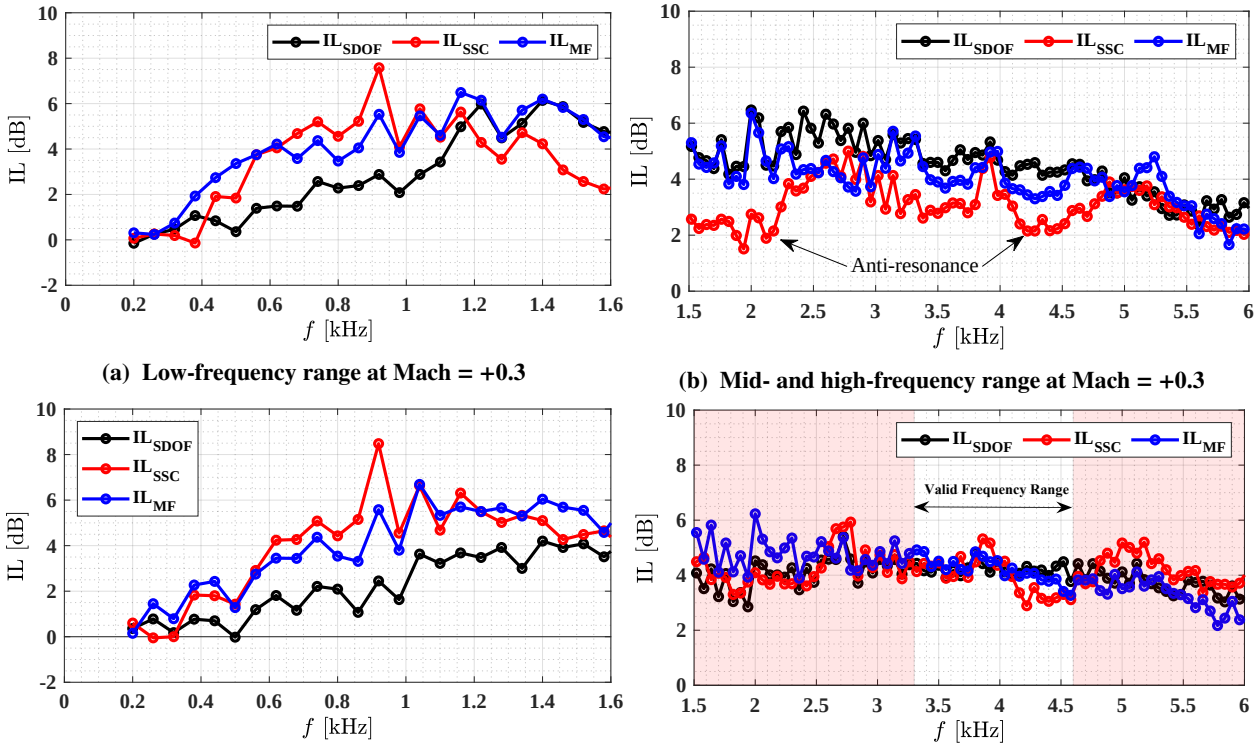

(a) Low-frequency range at Mach = +0.3

(b) Mid- and high-frequency range at Mach = +0.3

(c) Low-frequency range at Mach = +0.5

(d) Mid- and high-frequency range at Mach = +0.5

Fig. 8 Insertion loss of the SSC, MultiFOCAL, and SDOF perforate liners for downstream sound propagation.

The insertion loss of the novel liners broaden and improve with increasing Mach number. Significant noise reduction is observed at lower frequencies, below 1 kHz, where the conventional SDOF perforate is less effective. At Mach = +0.5, the MultiFOCAL and SSC liner concepts provide an insertion loss of at least 3 dB for frequencies between 0.5 and 2.2 kHz, with a maximum loss of 6 dB. In the mid-and high-frequency range, the MultiFOCAL concept continues to maintain attenuation levels comparable with the reference optimum SDOF perforate. The insertion loss of the SSC concept is valid only for frequencies between 3.3 and 4.6 kHz as the S/N_{dB} (> 4 dB) meets the acceptable criteria in that frequency range. As stated earlier, the insertion loss measurement results are not valid in the highlighted region for the SSC concept. Otherwise, the insertion loss of the SSC liner concept is comparable to the MultiFOCAL panel in the valid frequency ranges, except for a dip between 4 to 4.5 kHz.

Even though both novel liner panels were optimised at Mach = +0.3 and for SPL = 140 dB [9], it is clear that they can also provide improved attenuations at Mach = +0.5. As described in Ref.[9], the cavity depth of the SSC liner concept was also reduced to 20 and 40 mm. In addition, the porosity of the facing sheet and the slanted septum layers were optimised to achieve maximum insertion loss. A reduction in cavity depth shifted the insertion loss peak towards a higher frequency. However, the SSC always provides a significant increase in insertion loss at lower frequencies (below 1700 Hz) when compared against an optimised SDOF perforate while maintaining similar attenuation levels at higher frequencies.

B. Upstream propagation

The experimental insertion loss results for upstream sound propagation are presented in **Fig. 9**. From **Fig. 9a** and **Fig. 9c**, it can be seen that the insertion loss for upstream propagation at lower frequencies is generally higher than for downstream propagation. For instance, at Mach = −0.3, comparing the attenuation level of the novel liners with the traditional SDOF perforate concept, as shown in Fig. 9a, it is apparent that the broadband liners can provide an insertion loss in the NLR duct of up to 15-20 dB, for frequencies between 350 and 850 Hz. Furthermore, the peak insertion loss frequency for both the SSC and MultiFOCAL decreases with increasing Mach number. This shift in the frequency of

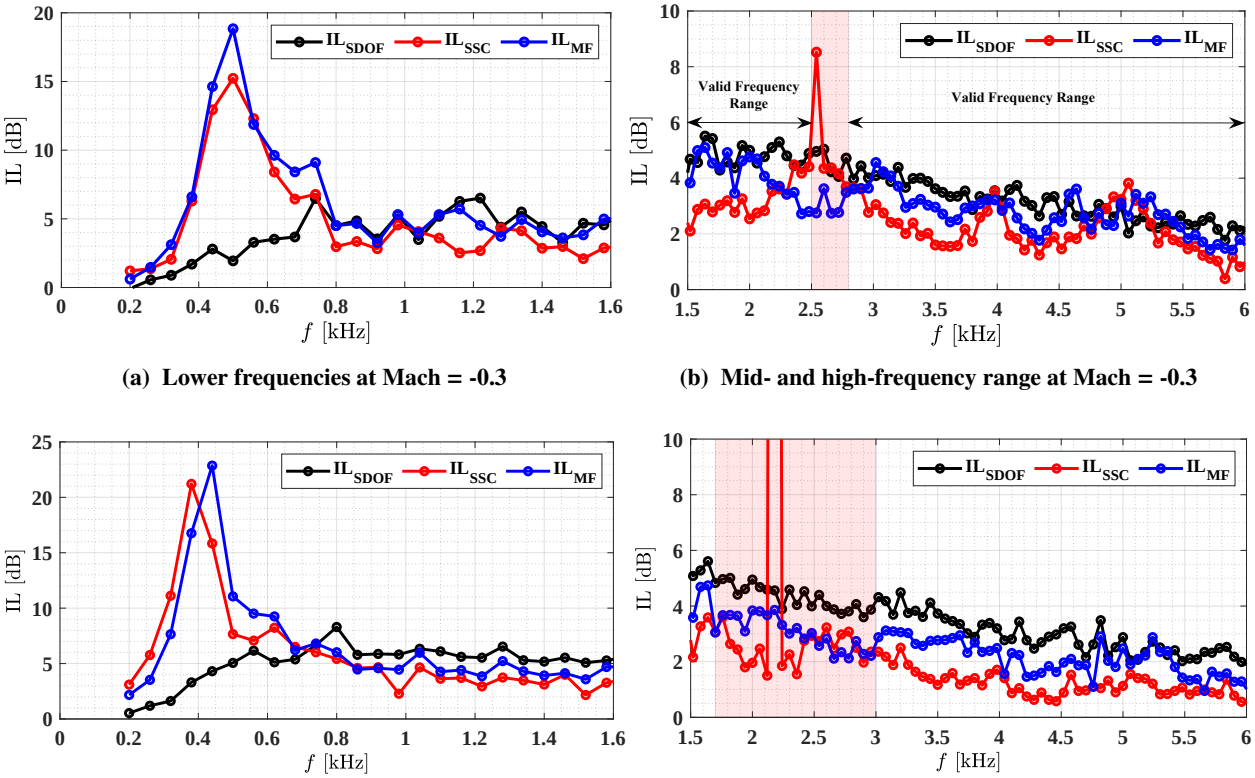

(a) Lower frequencies at Mach = -0.3

(b) Mid- and high-frequency range at Mach = -0.3

(c) Lower frequencies at Mach = -0.5

(d) Mid- and high-frequency range at Mach = -0.5

Fig. 9 Insertion loss of the SSC, MultiFOCAL, and SDOF perforate liners for upstream sound propagation.

peak attenuation can be seen by comparing the downstream and upstream spectra; this is due to the influence of the grazing flow direction and Mach number on the optimum wall impedance [9].

Above 1 kHz, the novel liner concepts are less efficient than the SDOF perforate (NLR reference panel). This is because the liners are optimised to provide maximum insertion loss at Mach = +0.3 and for SPL = 140 dB. Consequently, the liner geometrical parameters are tuned to match or fall as close as possible to the NLR flow duct optimum wall impedance for downstream propagation at Mach = +0.3, also noting that the higher than design POA of the novel liners leads to a relatively lower resistance and attenuation. The attenuation performance may be improved by re-optimisation for the upstream propagation case.

The insertion loss spectra in **Fig. 9b** and **Fig. 9d** show clearly the impact of the SSC liner self-noise. In the Mach = −0.3 insertion loss spectra, there is a small but distinct non-physical peak owing to liner self-noise generated by the background mean-flow, highlighted by the red shaded area. At Mach = −0.5, the effect of liner self-noise becomes much more evident. As indicated earlier, the SSC's self-noise arises due to the very low resistance provided by the manufactured panels compared to the designed target value. Both of the novel liner 3D printed panels have a relatively high manufactured percentage of open area due to larger than desired effective hole diameters, (the desired effective hole diameters and hence POAs may be realized through a further iteration of the 3D printing parameters). Additionally, the liner panels were tested at an OASPL value of 130 dB rather than the optimum design condition of 140 dB, also contributing to a relatively low panel resistance.

The effects of grazing flow Mach number on the acoustic impedance of the novel liner panels are difficult to estimate through measurements (in-situ method) due to their complex geometries. They may be extracted through an impedance eduction approach. However, pure tone impedance predictions were made using a COMSOL FE model with a sound pressure level of 130 dB at Mach numbers ranging from 0.3 to 0.7.

VI. Predicted insertion loss: Study on the effect of the boundary layer

In this section, the insertion loss predictions of the novel liners at Mach = 0.3 and 0.5 are compared with the measured insertion loss. Predictions are first made using a uniform-flow model since the absence of a boundary layer in the propagation model does not appreciably influence downstream predictions. However, for upstream predictions, boundary-layer effects can be significant, which are seen later in this paper in the prediction results.

The numerical model of the NLR flow duct used in this study was validated previously by comparing the predicted insertion loss of an SDOF linear liner with measurements. The validation results are reported in Ref. [9].

A. Tonal impedance with mean flow

Owing to the complex cavities, it was impossible to apply the in-situ impedance technique to measure the effect of grazing flow on the impedance of the SSC and MultiFOCAL concepts. Therefore, for both of the liner configurations, the tonal impedance values are predicted, including the grazing flow duct centreline Mach number effect, using the semi-empirical model developed by Murray and Astley [17]. **Fig. 10** shows the comparison of the predicted tonal

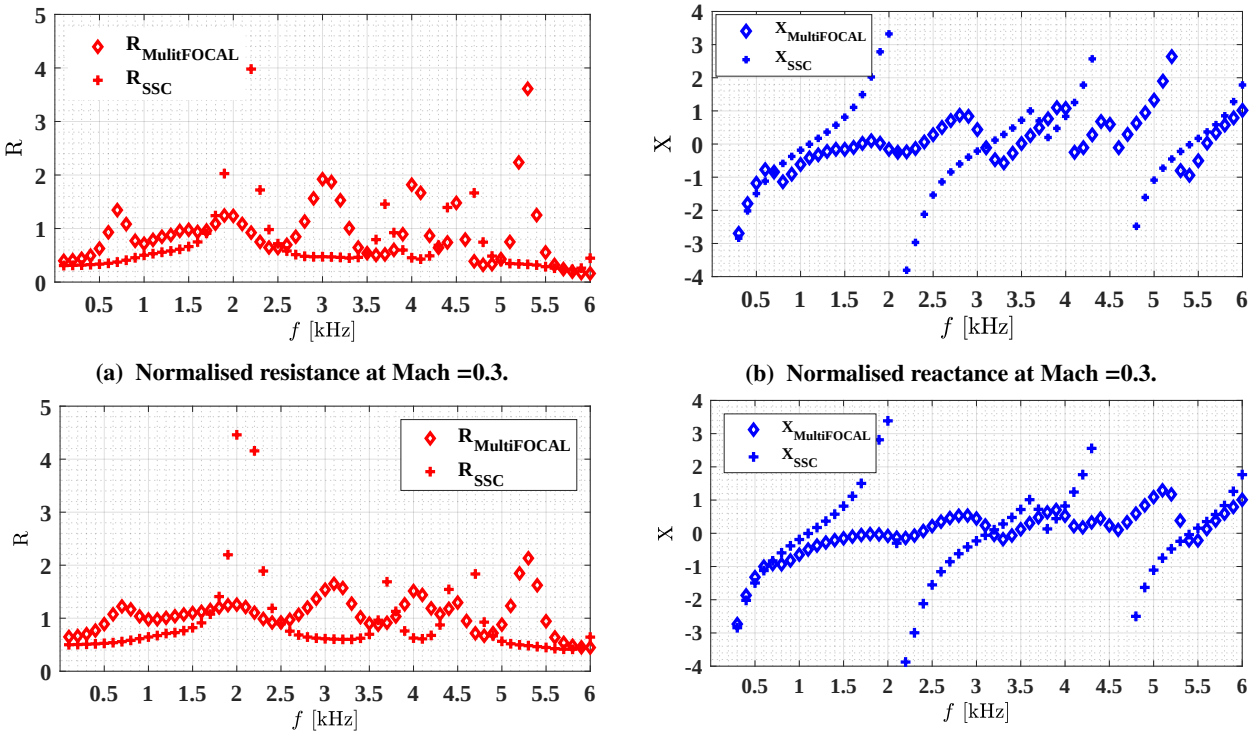

(a) Normalised resistance at Mach =0.3.

(b) Normalised reactance at Mach =0.3.

(c) Normalised resistance at Mach =0.5.

(d) Normalised reactance at Mach =0.5.

Fig. 10 Impedance spectra comparison between the SSC and the MultiFOCAL liner concepts for pure tone excitation at 130 dB and Mach = 0.3 and 0.5.

response for Mach = 0.3 and 0.5 for the SSC and MultiFOCAL liner concepts. Pure tone plane waves with frequency in the range from 100 to 6000 Hz (steps of 100 Hz), and at a sound pressure level of 130 dB, are normally incident on the liner face sheet.

Figure 10a and **10c** show the comparison of the predicted resistance for the SSC and the MultiFOCAL. In general, the normalised resistance of the SSC is lower than the MultiFOCAL. Comparison of **Fig. 10a** with **Fig. 6** and **Fig. 5** shows that the acoustic resistance increases for both of the liner configurations, with the largest increase mainly seen at low frequencies [18]. Owing to the presence of flow, a reduction of the effective orifice area causes an increase in the resistance, as numerically shown by Avallone and Damiano [19]. As the Mach number increases to 0.5, the maximum effect due to the SPL is approximately inversely proportionally to Mach number. This observation is consistent with the results previously reported by Murray and Astley [17] for an SDOF liner with a perforated facing sheet.

Figure 10b and **10d** show the comparison of the predicted reactance between the SSC and the MultiFOCAL. For the SSC liner panel, the predicted reactances do not vary with grazing flow. This is because of the relatively high open area in the manufactured liner panel. Note, also, that the resonance frequencies of the SSC liner concept do not change with increasing Mach number. For the MultiFOCAL liner panel, the predicted reactance decreases with grazing flow, especially at higher frequencies, and is "flattened" with increasing Mach number.

The predicted tonal impedance is used in the boundary condition for the grazing flow duct model. For a SPL of 130 dB, both liner panels are predicted to be weakly non-linear. The liner panels have a homogeneous impedance value throughout the lined section, with incident sound pressure level decaying along the axial direction from the liner panel's leading edge to its trailing edge. The non-linear component of these liners increases at high power settings, for example placed closer to the aero-engine fan, where the SPLs can be significantly higher than those measured in the NLR experimental facility.

As is the case with zero flow (**Fig. 6** and **Fig. 5**), **Fig. 10** once again shows that it is difficult to maintain the reactance spectrum of both of the novel liners close to zero, and to match the NLR duct optimum over a wide range of frequencies. The predicted insertion loss of the SDOF perforate, MultiFOCAL, and SSC show good agreement with the measurements at Mach = 0. These results are not shown here for brevity.

B. Downstream propagation: Uniform-flow model

As stated earlier, the insertion loss predictions are made for a frequency range from 100 Hz to 6000 Hz in steps of 100 Hz. The insertion loss was calculated by comparing the difference between the transmission loss with and without the liner panels installed in the duct, with flow grazing over the lined section to represent the NLR flow duct test conditions. A multi-modal broadband sound field is defined at the source plane using uncorrelated, cut-on,hard-wall radial duct modes, with equal acoustic power per mode.

First, for the downstream propagation, assuming that the boundary layer is infinitely thin, the standard Ingard–Myers [20] boundary condition is used and is given by,

$$\mathbf{u}\cdot\mathbf{n} = \frac{p}{Z} + \frac{1}{i\omega}\mathbf{u_o}\cdot\nabla\left(\frac{\mathbf{p}}{\mathbf{Z}}\right) - \frac{\mathbf{p}}{\mathbf{i}\omega\mathbf{Z}}\mathbf{n}\cdot(\mathbf{n}\cdot\nabla\mathbf{u_o})\,, \tag{2}$$

where $\mathbf{n}$ is the surface normal pointing out of the domain, and Z is the specific acoustic impedance of the liner. It should be noted that the impedance (Z) defined in Eqn.2 includes the effect of mean flow and sound pressure level (see Fig.10). **Fig. 11** and **Fig. 12** compare the predicted and the measured insertion loss of the SSC and the MultiFOCAL for Mach = +0.3 and +0.5, respectively. For both of the novel liner configurations, it is seen that the predicted insertion loss is in good agreement with the measurements. The prediction model for the SSC liner concept, (**Fig. 11**), captures the

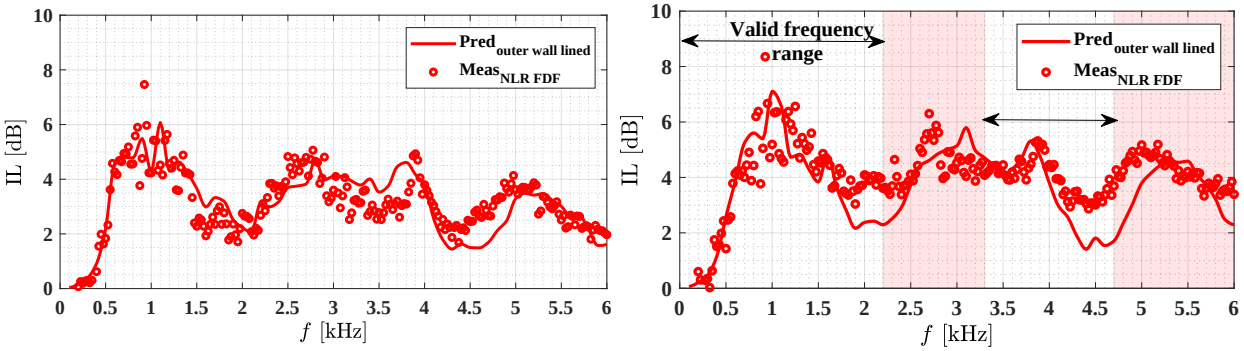

(a) Mach = +0.3 **(b) Mach = +0.5**

Fig. 11 Slanted Septum Core—Insertion loss comparison between the measurement and the prediction.

dips caused by anti-resonances. Also, it should be noted that these strong oscillations in the reactance curve can be dampened by exciting the SSC liner panel at a higher SPL and by reducing the facing sheet POA to the design value. For Mach = +0.5, the predicted insertion loss is still in good agreement with the measured data for most frequencies in the valid frequency range, showing discrepancies around 2.1 and 4.5 kHz near the anti-resonance of the liner. Unlike

tonal excitation, broadband excitation dampens the anti-resonance due to the interaction between the frequencies, which can also explain the small discrepancies between predicted and measured insertion loss at other frequencies. This observation has been verified by predicting the insertion loss using the normal incidence reactance curve obtained through measurements for broadband sound excitation. The results are not presented here for brevity.

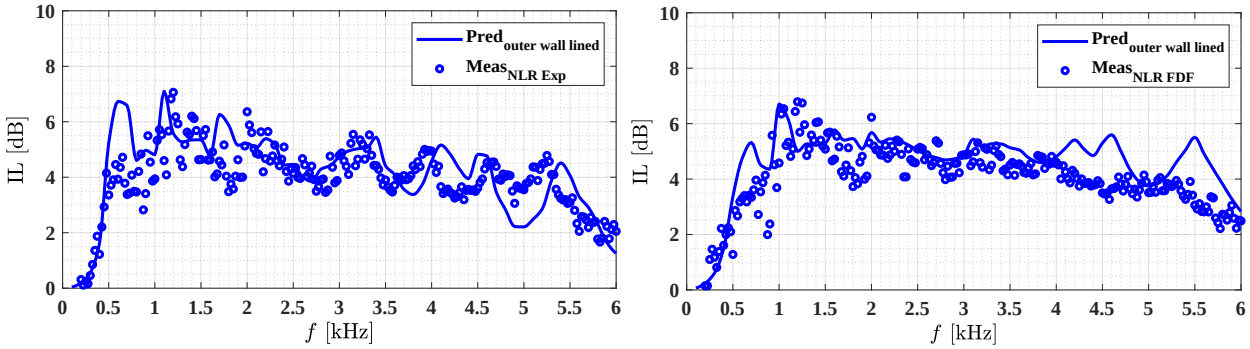

(a) Mach = +0.3 **(b) Mach = +0.5**

Fig. 12 MultiFOCAL—Insertion loss comparison between the measurement and the prediction.

Similar to the SSC panel, the predicted and measured insertion loss of the MultiFOCAL panel (Fig. 12) shows several oscillations in the spectra caused by the anti-resonances, especially for frequencies above 2.5 kHz, in line with the predicted impedance variations. Unlike the SSC, the reactance oscillations are not that strong for the MultiFOCAL. Therefore, the corresponding measured insertion loss of the liner has a relatively shallow dip in the spectrum with an overall insertion loss of 4 dB. From these results, it can be concluded that the boundary layer has negligible effects on the liner insertion loss for downstream sound propagation. Also, it is shown later in the paper that the insertion loss contours for downstream sound propagation with a uniform-flow model or a 1/4th power-law velocity profile are comparable at 400 Hz.

C. Upstream propagation: Sheared mean flow model

For the shear flow modelling, the results for the MultiFOCAL liner concepts are investigated in detail as the observations for the SSC concept are not expected to differ significantly from those for the MultiFOCAL.

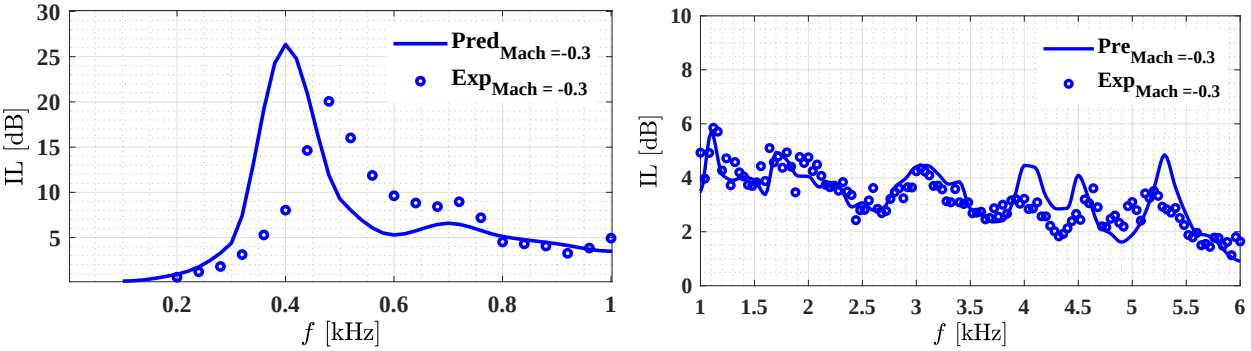

(a) Lower frequencies at Mach = -0.3 **(b) Higher frequencies at Mach = -0.3**

Fig. 13 MultiFOCAL—Insertion loss comparison between the measurement and the prediction with a uniform-flow model.

As shown in Fig. 13a, the insertion loss of the MultiFOCAL at Mach = 0.3 is over-predicted by 5-6 dB for upstream sound propagation with the uniform-flow model, especially around the peak attenuation at the lower frequencies. Additionally, there is also a slight shift in the frequency of the peak insertion loss, with a difference of 80 Hz. Similar to the measurement, the predicted insertion loss of the liner reduces drastically for frequencies between 0.5 to 0.8 kHz.

For frequencies between 0.8 to 1.6 kHz, the insertion loss stays constant at around 4 dB. Then, for frequencies above 2 kHz, the loss reduces gradually. More interestingly, for frequencies between 1 to 3.8 kHz, the predictions with the uniform flow are in good agreement with the measurements. The impact of boundary-layer refraction can be directly related to the location of the liner impedance on the R-X contour, with some frequencies more significantly affected than others. However, the disagreement in the insertion loss increases at higher frequencies. This may be because the liner response due to broadband excitation is slightly different from the predicted tonal response at higher frequencies.

The boundary-layer effect has been studied for upstream propagation based on model boundary-layer profiles presented in **Table. 2**. For this purpose, the linearised Euler equations frequency-domain interface in COMSOL is used for modelling sound propagation. Furthermore, the Pridmore-Brown equation is solved at the source plane for injecting the modal sound field with the corresponding axial wavenumbers.

In this study, the 1/4th power-law velocity profile is selected, in addition to the quarter-sine profile, for insertion loss predictions. The 1/4th power-law is a good approximation to the measured mean-flow profile in the NLR flow duct. The quarter-sine profile is useful as a simple model profile that includes shear flow. These two velocity profiles used in this study are shown in Fig.14a. The displacement thickness for both velocity profiles is matched and equals $\delta^* = 4.4$ mm.

Table 2 Model velocity profiles

Profile	$u_z(r)$		δ^*/δ
Quarter-Sine	$U \sin[(\pi/2)((r-r_i)/\delta)]$	$r_i \le r \le r_i + \delta$	
	U	$r_i + \delta \le r \le r_o - \delta$	$(\pi-2)/\pi$
	$U \sin[(\pi/2)((r_o-r)/\delta)]$	$r_o - \delta \le r \le r_o$	
1/4th Power-law	$U((r-r_i)/\delta))^{1/N}$	$r_i \le r \le r_i + \delta$	
	U	$r_i + \delta \le r \le r_o - \delta$	$1/(1+N)$
	$U((r_o-r)/\delta))^{1/N}$	$r_o - \delta \le r \le r_o$	

The boundary-layer region has thickness δ. Outside the boundary layer, the flow is assumed to be uniform, and it is defined by the free-stream velocity U. It is noted that, in the case of non-uniform flow, the mode shapes are not orthogonal. However, the calculation of the sound power loss is still performed assuming an incoherent sum as it has been shown by Brooks and McAlpine [21] that the interactions between different modes due to a non-uniform flow can be neglected.

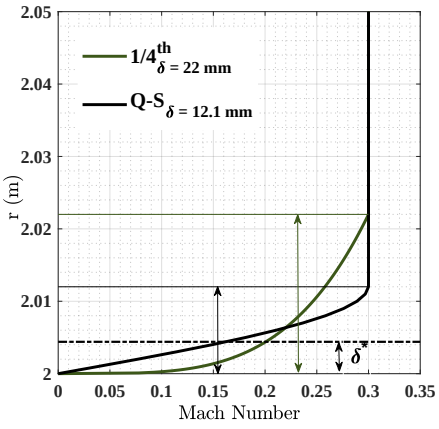

(a) (Blue line) 1/4th power-law, and (Black line) quarter-sine.

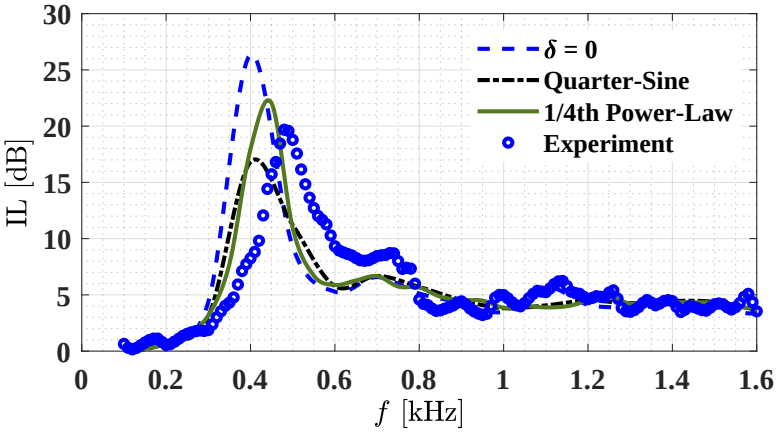

(b) Insertion loss of MultiFOCAL

Fig. 14 MultiFOCAL—Insertion loss comparison between the measurement and the prediction with a sheared mean flow model. (Blue line) Uniform flow, (Green line) 1/4th power-law, and (Black line) quarter-sine.

Fig. 14b shows a comparison of the predicted insertion loss spectra for the MultiFOCAL concept with 1/4th

power-law (δ = 22 mm) and quarter-sine (δ = 12.1mm) boundary-layer profiles. For comparison, the insertion loss prediction results for a uniform mean-flow (δ = 0) is also included along with the measured data. The boundary layer's clear impact on the predicted insertion loss, especially for frequencies between 0.3 and 0.8 kHz, can be seen. It can be seen that the predicted insertion losses corresponding to these two velocity profiles are substantially different, especially around the peak frequency region. Compared to uniform flow, the peak insertion loss of the MultiFOCAL concept, around 0.4 kHz, with a quarter-sine boundary layer profile (δ = 12.1 mm) reduces substantially by 10 dB. Also, there is a slight shift in the spectrum towards the measured data, clearly noticeable for frequencies below 0.4 kHz. With a 1/4th power-law profile, the peak has shifted to 0.45 kHz, and the peak loss value is reduced by 4 dB, showing improved agreement with the measured data. This indicates the insertion loss sensitivity near the optimum wall impedance to the type of boundary-layer velocity profile. For frequencies between 0.8 and 1.6 kHz, the insertion loss prediction with the 1/4th power-law collapses with the quarter-sine results and agrees well with the measurements.

Fig.15 shows the insertion loss contours varying the resistance from 0.001 ρc to 5ρc and varying the reactance from -5ρc to 5ρc, at 400 Hz and Mach = 0.3. From Figs. 15a and 15b, it can be seen that the effect of the boundary layer on the optimum resistance, reactance, and maximum attainable insertion loss is negligible at 400 Hz for downstream sound propagation. However, for upstream sound propagation (see Figs. 15c and 15d), although the optimum resistance and reactance values are comparable, there is a significant decrease in the maximum possible insertion loss by 4 dB. These

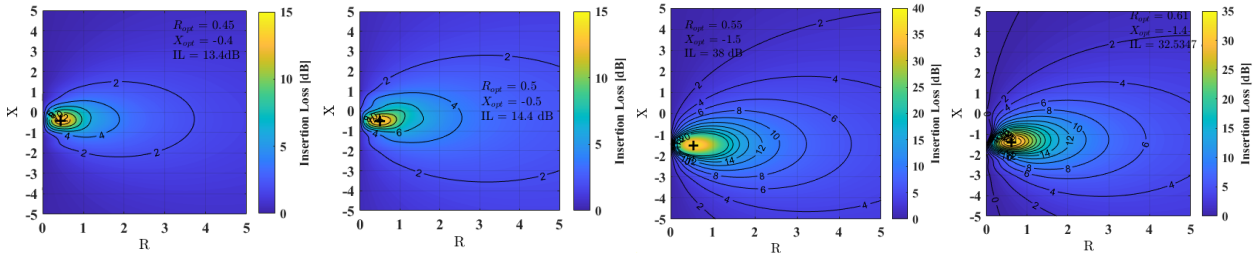

(a) Uniform flow M = +0.3 **(b) 1/4th Power-law M = +0.3** **(c) Uniform flow M = -0.3** **(d) 1/4th Power-law M = -0.3**

Fig. 15 Insertion loss contour plots for the NLR flow duct with a single wall lined.

results show, for upstream propagation, that the boundary-layer profile and its thickness affects the maximum attainable insertion loss for impedance values near the wall optimum impedance. Also, away from the optimum, the attenuation is reduced for a given impedance. Further development of this shear-flow modelling for upstream sound propagation will be presented in detail in a future paper using measured velocity profiles from the NLR flow duct facility.

VII. Liner self-noise

In the presence of grazing mean flow, the SSC liner panels generate undesirable strong tones that affect the measured insertion loss spectra, as already seen earlier in the paper. Tam et al. [22] has shown that for a typical SDOF perforate liner, unsteady flow vortices in the shear layer are formed near the upstream edge of the facing sheet orifice opening. These vortices convect downstream of the orifice and impact with the downstream edge. This generates acoustic waves that travel upstream to induce vertical motion in the shear layer, driving a feedback loop leading to amplification of the generated sound (often related to Rossiter-type feedback mechanisms [23]). For brevity, further details about this phenomenon are not presented here and are available in Ref.[23]. However, the typical frequency for such tones has been predicted to be as high as 30 kHz for the orifice dimensions desirable for aero-engine linings [22].

In order to study the source of self-noise from flow over the novel liner configurations, especially the SSC liner concept, pressure measurements were made inside the flow duct at seven locations as shown in **Fig.16**. The in-duct pressure measurements were made for Mach numbers ranging from 0.3 to 0.7. **Figure 17** shows the sound pressure level spectra measured inside the NLR flow duct by microphones flush-mounted on the wall opposite the lined section at locations 1, 3, and 6. In **Fig.17a**, at Mach = 0.3, two dominant peaks with a sound pressure level of 105 dB and 97 dB are generated by the flow over the baseline SSC liner, at 1.26 and 2.3 kHz. With increasing Mach number, the peaks are shifted accompanied by an overall increase in the sound pressure level. For example, at Mach = 0.5, the first peak is at 2.3 kHz, and the amplitude has increased by 10 dB over the value at Mach = 0.3. Additionally, the sound pressure level of the SSC liner configuration with a reduced POA (15.9 %) for the face sheet shows a considerable

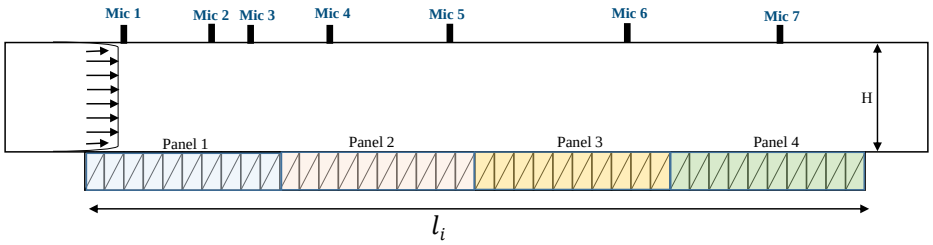

Fig. 16 Linear in-duct microphone array.

reduction in the amplitude. This highlights that the self-noise generated by the SSC liner concept is related to the low resistance of the face sheet due to the manufactured high open area. In Fig.17b and Fig.17c, similar comparisons are made for the SSC liner panels with facing sheet POAs of 27.2 and 15.9 % at microphone locations 3 and 6. Comparing the sound pressure level of the SSC liner panel with a facing sheet POA of 27.2 %, Figs.17a–17c show that there is a decrease in the tonal amplitude from the leading to the trailing edge of the liner panel. This suggests that the growing boundary-layer affects the feedback mechanism responsible for the SSC liner self-noise.

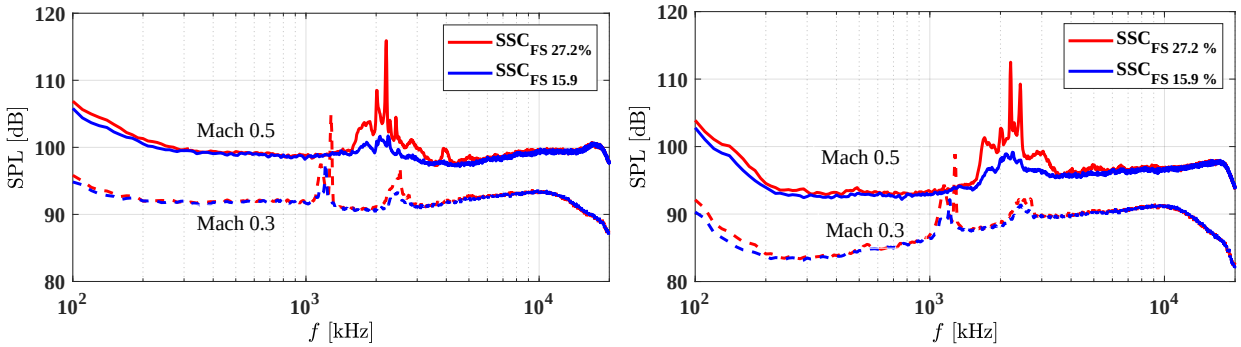

(a) Microphone 1

(b) Microphone 3

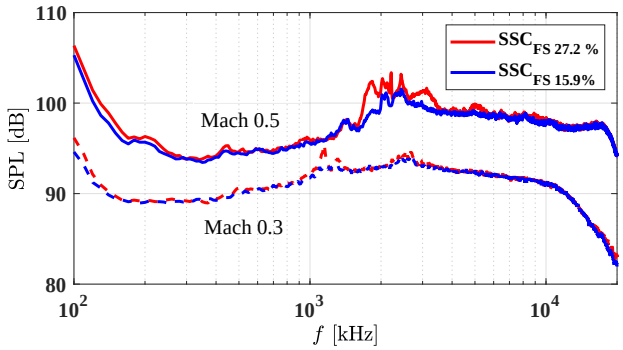

(c) Microphone 6

Fig. 17 SSC—Induct pressure measurements at microphone locations 1, 3 and 6 on the wall opposite to the lined surface.

From Fig.17 it can be noticed that the frequencies associated with liner self-noise are related to the flow Mach number, especially the first peak. These frequencies can be predicted using the feedback model proposed by Rossiter [23], given by

$$f_l^r = \frac{U}{L}\frac{m-\alpha}{1/K_c + M}, \tag{3}$$

where $m = 1,2,3\ldots$ is the mode number, L is the cavity width, $\alpha = 0.25$ is the empirical constant which increases as L/D increases, K_c is the ratio of the vortex convection speed across the liner cavity face sheet to the free-stream

velocity, and M is the free-stream Mach number.

Unlike the case of Eq.3 proposed by Rossiter, Block [24] has shown that the self-sustained oscillation frequencies in deep cavities are also sensitive to the L/D ratio of the cavity in addition to the Mach number, and it is given by [25],

$$f_l^b = \frac{U}{L} \frac{m}{1/K_c + M(1 + \frac{0.514}{L/D})}, \tag{4}$$

where m is the mode number, and $K_c = 0.57$.

Fig.18 shows the comparison of liner self-noise peak frequencies measured at microphone location 1 with the predicted self-sustained oscillation frequencies for the first three modes from Eq.3 and Eq.4. The value of K_c used here is for a typical open cavity. The agreement of the liner self-noise frequencies with Eqs.3 and 4 shows that the liner face sheet can be 'transparent' if the POA is very high, and consequently offers less resistance to dampen the self noise.

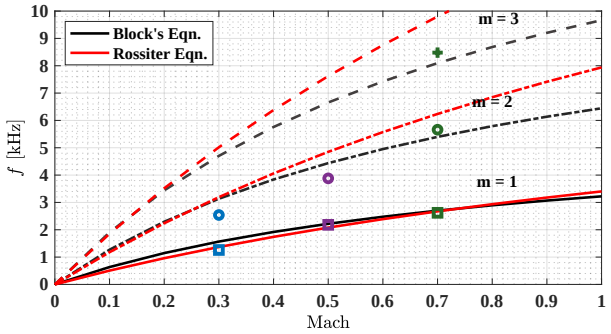

Fig. 18 Liner self-noise frequencies.

Fig.19 shows the comparison of the flow noise measurement at microphone location 1 for the SSC and MultiFOCAL. Unlike the SSC liner concept, the MultiFOCAL liner does not generate any strong tones, as can be seen from the figure. This draws the same conclusion regarding the relationship between the liner face-sheet resistance and self noise, driven also by the POA of the liner's facing sheet rather than just the hole diameter or cavity width alone.

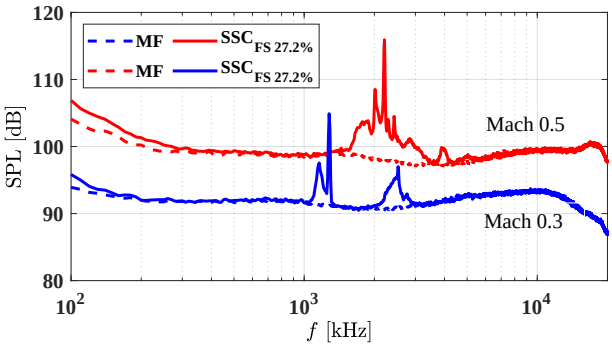

Fig. 19 Microphone 1

VIII. Conclusion

This paper presents the results from a detailed numerical and experimental study into the broadband sound attenuation performance of two novel liners. These include a slanted septum core with varying percentage open area, and a multiple folded cavity acoustic liner. First, the normal incidence tonal response of the novel broadband liner concepts is predicted and measured without grazing mean flow. The predicted normal incidence impedance spectra without grazing flow agree well with measurements, thus giving confidence in the modelling, manufacturability, and predicted performance of the proposed novel liners. It is also shown that the sound absorption capability of the optimised novel liners is

predicted and measured to be more broadband when the incident sound pressure level is increased, due to an increase in resistance, and a reduction in reactance, over a wide range of frequencies. The slanted septum core is shown to provide broadband sound absorption by varying the porosity of the diagonal layers l_1 and l_2, combining the benefit of the deep liner at low frequency, and a complex double-degree of freedom liners at higher frequencies, while the MultiFOCAL concept enhances the broadband attenuation by varying the impedance over the facing sheet.

The effect of mean flow on the liner insertion loss is predicted and analysed in detail, including modelling the impact of boundary-layer refraction by considering the influence of the type of boundary-layer velocity profile, thickness, and its impact on the optimum liner impedance. For downstream sound propagation, representative of an aero-engine bypass duct, a simple convected wave equation model with the standard Ingard–Myers boundary condition is sufficient to predict the liner attenuation accurately, confirming that the effect of boundary layers can be neglected.

However, for upstream sound propagation with a uniform mean-flow model, the insertion loss is over-predicted by up to 5-6 dB compared to the experimental data. This shows the importance of boundary-layer effects in numerical modelling of upstream propagation. The optimum impedance and the corresponding maximum insertion loss at lower frequencies are sensitive to the mean-flow Mach number, flow direction and boundary-layer profile. The fully resolved boundary-layer model uses the linearised Euler equations to examine the effect of the boundary layer on the predicted liner attenuation for upstream propagation, which improves the results compared to the predictions obtained with uniform flow.

This study also shows that the effect of flow direction on the liner impedance is negligible. Instead, the liner impedance's location relative to the R-X contours gives different predicted attenuation values for either upstream or downstream sound propagation. Additionally, it has been shown that the quarter-sine and 1/4th power-law boundary-layer profiles with constant displacement thickness predict different attenuation levels at lower frequencies. Further studies will be carried out to investigate this.

The experimental results show that the SSC liner's facing sheet (with POA of 27.2%) becomes almost transparent and still allows the cavity width-wise self-sustained oscillations to exist, thereby generating strong tones which affect the measured insertion loss. In addition, the strength of the self-noise tone decays with the growing boundary layer, and it is damped as the face-sheet resistance increases, which is controlled by the percentage of open area.

Acknowledgments

The work in this paper is part of the ARTEM project. This project has received funding from the European Union's Horizon 2020 research and innovation programme under grant No. 769 350. The authors wish to acknowledge the technical input to this work from Dr. Rie Sugimoto (ISVR), and Prof. Jeremy Astley (ISVR), as well as Dr. Daisuke Sasaki (Kanazawa Institute of Technology). Also the authors wish to acknowledge the continuing support provided by Rolls–Royce plc through the University Technology Centre in Propulsion Systems Noise at the Institute of Sound and Vibration Research.

References

[1] Sugimoto, R., Murray, P., and Astley, R., "Folded Cavity Liners for Turbofan Engine Intakes," *American Institute of Aeronautics and Astronautics, 18th AIAA/CEAS Aeroacoustics Conference*, 2012.

[2] Schiller, N. H., and Jones, M. G., "Smeared Impedance Model for Variable Depth Liners," *American Institute of Aeronautics and Astronautics, AIAA/CEAS Aeroacoustics Conference*, 2018.

[3] Nayfeh, A. H., "Effect of the acoustic boundary layer on the wave propagation in ducts," *The Journal of the Acoustical Society of America*, Vol. 54, No. 6, 1973, pp. 1737–1742. https://doi.org/10.1121/1.1914472.

[4] Nayfeh, A. H., Kaiser, E., J, and Shaker, S., B, "Effect of mean-velocity profile shapes on sound transmission through two-dimensional ducts," *Journal of Sound and Vibration*, Vol. 34, No. 3, 1974, pp. 413–423.

[5] Myers, M., "On the acoustic boundary condition in the presence of flow," *Journal of Sound and Vibration*, Vol. 71, No. 3, 1980, pp. 429 – 434. https://doi.org/https://doi.org/10.1016/0022-460X(80)90424-1.

[6] Ingard, U., "Influence of Fluid Motion Past a Plane Boundary on Sound Reflection, Absorption, and Transmission," *The Journal of the Acoustical Society of America*, Vol. 31, No. 7, 1959, pp. 1035–1036.

[7] Gabard, G., "Boundary layer effects on liners for aircraft engines," *Journal of Sound and Vibration*, Vol. 381, 2016, pp. 30–47.

[8] Brambley, E. J., "Well-Posed Boundary Condition for Acoustic Liners in Straight Ducts with Flow," *AIAA Journal*, Vol. 49, No. 6, 2011, pp. 1272–1282. https://doi.org/10.2514/1.J050723.

[9] Palani, S., Murray, P., McAlpine, A., and Richter, C., "Optimisation of slanted septum core and multiple folded cavity acoustic liners for aero-engines," *AIAA AVIATION 2021 FORUM*, 2021, pp. 1–17. https://doi.org/10.2514/6.2021-2172, URL https://arc.aiaa.org/doi/abs/10.2514/6.2021-2172.

[10] COMSOL, "Acoustics module user's guide," *Version 5.3a*, 2017.

[11] Murray, P., Ferrante, P., and Scofano, A., "Influence of Aircraft Nacelle Acoustic Panel Drainage Slots on Duct Attenuation," *13th AIAA/CEAS Aeroacoustics Conference (28th AIAA Aeroacoustics Conference)*, 2007. https://doi.org/10.2514/6.2007-3548.

[12] Scofano, A., Murray, P., and Ferrante, P., "Back-Calculation of Liner Impedance Using Duct Insertion Loss Measurements and FEM Predictions," *13th AIAA/CEAS Aeroacoustics Conference (28th AIAA Aeroacoustics Conference)*, 2007. https://doi.org/10.2514/6.2007-3534.

[13] Eversman, W., "Broadband noise suppression for turbofan inlet applications," *International Journal of Aeroacoustics*, Vol. 15, No. 4-5, 2016, pp. 367–394. https://doi.org/10.1177/1475472X16642131.

[14] McAlpine, A., Astley, R., Hii, V., Baker, N., and Kempton, A., "Acoustic scattering by an axially-segmented turbofan inlet duct liner at supersonic fan speeds," *Journal of Sound and Vibration*, Vol. 294, No. 4, 2006, pp. 780–806. https://doi.org/https://doi.org/10.1016/j.jsv.2005.12.039.

[15] Morfey, C., "Sound transmission and generation in ducts with flow," *Journal of Sound and Vibration*, Vol. 14, 1971, pp. 37–55. https://doi.org/10.1016/0022-460X(71)90506-2.

[16] Palani, S., Murray, P., McAlpine, A., Sasaki, D., and Richter, C., "Slanted septum and multiple folded cavity liners for broadband sound absorption," *International Journal of Aeroacoustics*, Vol. 20, No. 5-7, 2021, pp. 633–661. https://doi.org/10.1177/1475472X211023835, URL https://doi.org/10.1177/1475472X211023835.

[17] Murray, P., and Astley, R., "Development of a single degree of freedom perforate impedance model under grazing flow and high SPL," *18th AIAA/CEAS Aeroacoustics Conference (33rd AIAA Aeroacoustics Conference)*, 2012.

[18] Zhang, Q., and Bodony, D., "Direct Numerical Simulation of Three Dimensional Honeycomb Liner with Circular Apertures," *AIAA*, 2010.

[19] Avallone, F., and Damiano, C., "Acoustic-induced velocity in a multi-orifice acoustic liner grazed by a turbulent boundary layer," *AIAA AVIATION 2021 FORUM*, 2021, pp. 1–13. https://doi.org/10.2514/6.2021-2169, URL https://arc.aiaa.org/doi/abs/10.2514/6.2021-2169.

[20] Myers, M., "On the acoustic boundary condition in the presence of flow," *Journal of Sound and Vibration*, Vol. 71, No. 3, 1980, pp. 429–434.

[21] Brooks, C., and McAlpine, A., "Sound transmission in ducts with sheared mean flow," *13th AIAA/CEAS Aeroacoustics Conference (28th AIAA Aeroacoustics Conference)*, 2007. https://doi.org/10.2514/6.2007-3545.

[22] Tam, C. K., Pastouchenko, N. N., Jones, M. G., and Watson, W. R., "Experimental validation of numerical simulations for an acoustic liner in grazing flow: Self-noise and added drag," *Journal of Sound and Vibration*, Vol. 333, No. 13, 2014, pp. 2831–2854. https://doi.org/https://doi.org/10.1016/j.jsv.2014.02.019.

[23] Rossiter, J. E., "Wind-tunnel experiments on the flow over rectangular cavities at subsonic and transonic speeds," *Ministry of Aviation, Reports, and Memoranda*, Vol. 3438, 1964, pp. 1–32.

[24] Block, P. J. W., "Noise response of cavities of varying dimensions at subsonic speeds," *NASA TN D-8351*, 1976, pp. 1–34.

[25] Bozak, R., Jones, M., Howerton, B., and Brown, M., "Effect of Grazing Flow on Grooved Over-the-Rotor Acoustic Casing Treatments," *25th AIAA/CEAS Aeroacoustics Conference*, 2019, pp. 1–17. https://doi.org/10.2514/6.2019-2564.